

Supplementary Materials: Study of K-Feldspar and Lime Hydrothermal Reaction: Phase and Mechanism with Reaction Temperature and Increasing Ca/Si Ratio

Shanke Liu, Cheng Han, and Jianming Liu

Element Content and QPA

The element content in the filtrated solutions of L-1 to L-6 and M-1 to M-9 is shown as the form of $\text{mg}\cdot\text{L}^{-1}$ in Table S3. For comparison, the corresponding element contents calculated from the XRPD results are also listed in Table S3. In fact, QPA results were based on XRPD data (Table S2). For convenience, the authors defined the contents from XRPD instead of the QPA results. The contents calculated from XRPD in Table S3 covered all phases with the exception of K-feldspar to compare with those determined by ICP-OES (all elements determined by ICP-OES are from those phases dissolved in $0.5 \text{ mol}\cdot\text{L}^{-1}$ HCl except K-feldspar). The ACSH content was approximately obtained from the difference of four oxide sums ($\text{K}_2\text{O} + \text{SiO}_2 + \text{Al}_2\text{O}_3 + \text{CaO}$, the oxide contents were calculated from their corresponding element contents) dissolved in $0.5 \text{ mol}\cdot\text{L}^{-1}$ HCl, and these four sums calculated from XRPD and QPA data were normalized. Therefore, only normalized QPA data are listed here. A plot of the element contents determined by ICP-OES versus those calculated from XRPD is shown in Figure S5.

We described and discussed the solubility of the elements (K, Si, Al, and Ca) and the phases (tobermorite, grossular, alpha-dicalcium silicate hydrate, amorphous calcium silicate hydrate, potassium carbonate, bütschliite, calcite, calcium hydroxide, and leftover K-feldspar) in the previous work [1], and therefore we do not state them here.

The element content results from XRPD are in agreement with those from ICP-OES (Figure S5(a), Pearson's $r = 0.9887$; Figure S5(b), Pearson's $r = 0.9893$), proving that the quantitative phase results obtained from the XRPD data were reliable. However, some values from the XRPD data slightly deviated from the ICP-OES results, especially for the Si content of the samples L-4 and M-5. In theory, the element contents from XRPD should have been equal to those dissolved in $0.5 \text{ mol}\cdot\text{L}^{-1}$ HCl. The deviation may have been caused by the application of inaccurate chemical formula of formed phases and may have been introduced by the approximate estimation of ACSH content.

Nomenclature of Grossular and Hydrogarnet

Hydrogarnet is also known by different names including hibschite, katoite, plazolite, grossularoid, garnetoid, and hydrogrossular. Based on the analysis of XRPD, we attributed the phase of hydrogarnet to hibschite ($\text{Ca}_3\text{Al}_2(\text{SiO}_4)_{1.53}(\text{OH})_{5.88}$, PDF card number 01-075-1690). However, the name hibschite (former formula: $\text{Ca}_3\text{Al}_2(\text{SiO}_4)_{3-x}(\text{OH})_{4x}$, where $x = 0.2-1.5$) was discredited in favor of grossular, as Si is the dominant cation at the Z site in the recent report published by International Mineralogical Association (IMA) [2]. Therefore, we replaced "hibschite" with the new nomenclature "grossular". Based on the calculation, x reaches 2 for the hydrogarnet phase in the sample M-9 (Table S5), and then the hydrogarnet phase should be katoite. However, for brevity, only "grossular" or "hydrogarnet" was used in the text.

Definition of the Percentage of K-feldspar Dissolution (D , %)

The percentage of K-feldspar dissolution (D , %) was approximately calculated from the

following equation:

$$D\% = \frac{\text{Dissolved K – feldspar}}{\text{Mass of K – feldspar}} \times 100 = \frac{S_{K_2O+SiO_2+Al_2O_3}}{55} \times 100$$

wherein $S_{K_2O+SiO_2+Al_2O_3}$ is the oxide sum of K, Si, Al dissolved in 0.5 mol·L⁻¹ HCl (the oxide contents were calculated from their corresponding element contents), and 55 is the weight percent of K-feldspar in the solid mixture of K-feldspar powder (5.5 g) and lime powder (4.5 g) before the hydrothermal reaction. The authors did not consider the change of about 10% solid mass after the hydrothermal reaction due to water insertion in the silicate structure and carbonatization during vaporizing water. Therefore, the percentage of K-feldspar dissolution (D , %) was an approach, but the approach did not affect the conclusions. The percent of K-feldspar dissolution, along with the original data of plotting Figure 9, are listed in Table S7.

Table S1. Overview of the hydrothermal reaction with reactant ratio ($T = 190\text{ }^\circ\text{C}$, $t = 13.6\text{ h}$, and $V_{\text{deionized water}} = 30\text{ mL}$).

Samples	K-feldspar/g	Lime/g	Atom mole ratio			
			N _{Ca/Si}	N _{Ca/Al}	N _{Ca/(Al+Si)}	N _{Al/Si}
M-1	7.0	3.0	0.72	2.16	0.54	0.33
M-2	6.5	3.5	0.90	2.78	0.68	0.33
M-3	6.0	4.0	1.12	3.36	0.84	0.33
M-4	5.5	4.5	1.37	4.15	1.03	0.33
M-5	5.0	5.0	1.68	5.04	1.26	0.33
M-6	4.5	5.5	2.05	6.19	1.54	0.33
M-7	4.0	6.0	2.52	7.56	1.89	0.33
M-8	3.5	6.5	3.12	9.36	2.34	0.33
M-9	3.0	7.0	3.91	11.85	2.94	0.33

Table S2. Quantitative phase analysis by the Rietveld method (%).

Sample	R factors					K-feldspar	Calcium hydroxide	Calcite	Grossular
	R_{wp}	R_p	R_{exp}	χ^2	R_r^2	KAlSi ₃ O ₈	Ca(OH) ₂	CaCO ₃	Ca ₃ Al ₂ (SiO ₄) _{1.53} (OH) _{5.58}
L-1	16.8	12.8	10.7	2.45	9.59	54.35	34.60	6.13	/
L-2	15.7	12.0	10.9	2.09	8.60	49.80	29.90	8.72	1.12
L-3	14.8	11.3	11.0	1.80	7.32	40.69	22.83	9.45	12.50
L-4	15.7	12.3	11.2	1.97	12.1	16.33	/	16.58	18.33
L-5	16.8	13.0	11.1	2.28	14.4	9.53	/	3.86	25.56
L-6	19.2	14.8	11.0	3.03	10.8	7.00	/	2.62	24.56
M-1	15.0	11.6	10.9	1.9	7.92	42.05	/	3.56	14.76
M-2	15.1	11.7	11.0	1.9	9.60	35.14	/	4.29	16.93
M-3	15.1	11.7	11.0	1.9	9.61	28.20	/	3.97	20.95
M-4	15.3	12.0	11.1	1.9	10.7	21.25	/	7.15	23.95
M-5	15.5	12.1	11.2	1.9	8.84	24.75	7.36	13.94	16.51
M-6	15.7	12.3	11.4	1.9	9.29	20.40	11.33	16.47	20.48
M-7	16.3	12.7	11.5	2.0	9.69	17.10	19.85	18.44	19.19
M-8	16.1	12.5	11.7	1.9	8.88	13.63	26.00	14.92	17.74
M-9	17.0	13.3	11.5	2.2	9.65	13.46	36.21	10.23	18.96
Sample	α -C ₂ SH (alpha-dicalcium silicate hydrate)					Tobermorite	Potassium carbonate	Bütschliite	ACSH
	Ca ₂ (SiO ₃ OH)(OH)					Ca _{2.25} (Si ₃ O _{7.5} (OH) _{1.5})(H ₂ O)	K ₂ CO ₃	K ₂ CaCO ₃	
L-1	/					/	/	/	4.92

L-2	/	/	0.66	/	9.80
L-3	/	/	4.58	/	9.95
L-4	10.36	1.13	/	9.12	28.15
L-5	/	35.97	/	8.63	16.45
L-6	/	41.33	/	12.70	11.79
M-1	/	26.89	/	5.32	7.41
M-2	/	29.16	/	8.40	6.07
M-3	/	30.06	/	8.98	7.84
M-4	10.11	22.90	/	9.01	5.63
M-5	10.44	/	/	7.74	19.25
M-6	15.00	/	/	7.72	8.62
M-7	17.15	/	/	4.22	4.04
M-8	19.13	/	/	5.40	3.18
M-9	14.08	/	/	4.76	2.30

Note: “/” denotes that the phase did not form, i.e., the phase weight percent was 0%.

Table S3. Element contents measured by ICP–OES and calculated from XRPD.

Sample	Measurement by ICP-OES								Calculation from XRPD (mol·L ⁻¹)			
	Element contents in deionized water (mol·L ⁻¹)				Element contents in 0.5 mol·L ⁻¹ HCl (mol·L ⁻¹)				K	Si	Al	Ca
	K	Si	Al	Ca	K	Si	Al	Ca				
L-1	23.24	3.74	3.18	791.88	32.38	86.48	30.70	2404.23	0.00	0.00	0.00	2226.99
L-2	86.34	2.80	2.65	725.41	108.75	263.64	87.32	2442.11	41.51	12.62	15.88	2217.70
L-3	182.63	4.21	2.65	643.22	201.73	478.19	151.89	2422.81	288.06	143.50	180.47	2194.11
L-4	400.13	24.77	2.12	22.87	462.39	1075.59	342.42	2477.13	415.08	512.32	331.83	2526.44
L-5	411.75	24.77	1.59	20.01	604.35	1417.75	438.21	2462.12	337.87	1287.80	397.46	2399.94
L-6	419.23	12.62	2.65	20.01	689.03	1593.98	502.25	2484.28	470.70	1345.30	362.00	2424.96
M-1	263.16	28.98	0.53	17.15	368.59	910.11	284.73	1623.79	187.93	868.78	207.19	1693.48
M-2	302.17	36.46	0.53	16.44	394.32	939.09	304.31	1860.35	292.19	922.82	234.23	1841.75
M-3	339.5	49.55	0.53	16.44	433.34	1039.12	336.60	2171.96	318.33	1010.79	295.45	2053.66
M-4	366.10	89.28	0.53	17.87	472.36	1070.91	360.41	2367.78	312.12	996.95	329.89	2409.21
M-5	364.44	9.35	2.65	108.63	425.04	1075.59	369.94	2592.91	313.10	609.32	265.81	2815.91
M-6	338.70	5.14	2.65	196.54	352.81	873.65	273.62	2838.05	276.17	560.60	291.29	2990.29
M-7	307.16	4.21	3.70	542.45	322.10	739.49	246.63	3036.74	143.81	511.44	259.96	3331.61
M-8	288.06	3.27	3.70	602.49	303.84	717.99	232.87	3294.74	182.37	513.03	238.13	3548.40
M-9	236.59	3.27	3.70	657.52	253.20	621.70	197.41	3514.87	159.17	438.14	252.29	3687.66

Note: Element contents from XRPD were calculated from their corresponding the oxide contents in terms of QPA data.

Table S4. PDF data of hydrogarnet used in Figure 4a.

Chemical formula	Si content	Lattice parameter <i>a</i> (Å)	PDF card number
Ca ₃ Al ₂ (SiO ₄) ₃	3.00	11.8493	00-039-0368
Ca ₃ Al ₂ (SiO ₄) ₃	3.00	11.8500	01-084-1349
Ca ₃ Al ₂ (SiO ₄) _{2.16} (OH) _{3.36}	2.16	11.9400	01-072-0071
Ca ₃ Al ₂ (SiO ₄) ₂ (OH) ₄	2.00	12.0000	00-031-0250
Ca ₃ Al ₂ (SiO ₄) ₂ (OH) ₄	2.00	12.0400	00-042-0570
Ca ₃ Al ₂ (SiO ₄) _{1.53} (OH) _{5.88}	1.53	12.1740	01-075-1690
Ca ₃ Al ₂ (SiO ₄) _{1.25} (OH) ₇	1.25	12.2875	00-045-1447
Ca ₃ Al ₂ (SiO ₄)(OH) ₈	1.00	12.3580	00-038-0368
Ca _{2.93} Al _{1.97} Si _{0.64} O _{2.56} (OH) _{9.44}	0.64	12.3800	01-084-0917

Ca ₃ Al ₂ (OH) ₁₂	0.00	12.5727	00-024-0217
Ca ₃ Al ₂ (OH) ₁₂	0.00	12.5755	01-071-0735

Table S5. Estimated Si content, *x*, and Al/Si ratio of formed hydrogarnet from Equation (1) in this study.

Samples	Lattice parameter <i>a</i> (Å)	Si content	<i>x</i>	Al/Si
M-1	12.2028	1.44	1.56	1.39
M-2	12.2156	1.39	1.61	1.44
M-3	12.2138	1.39	1.61	1.44
M-4	12.1951	1.47	1.53	1.36
M-5	12.2231	1.36	1.64	1.47
M-6	12.2385	1.30	1.70	1.54
M-7	12.2563	1.23	1.77	1.63
M-8	12.2570	1.23	1.77	1.63
M-9	12.3174	0.99	2.01	2.01

Note: Lattice parameter *a* was obtained from the output data of QPA by the Rietveld method.

Table S6. EDS data of spherical and laminar particle in the sample L-6.

Sample L-6	Atom number determined by EDS	Ca:Si	Ca:Al	Ca:Al+Si	Al:Si
spherical particle	Ca _{2.72} K _{0.40} Al _{1.68} Si _{2.73} O _{17.75}	1:1	1.63:1	1:1.62	1:1.63
laminar particle	Ca _{2.50} K _{0.84} Al _{1.02} Si _{3.45} O _{17.19}	1:1.38	2.46:1	1:1.79	1:3.40

Note: The atom numbers were directly calculated from their corresponding weight percent determined by EDS.

Table S7. Percentage of K-feldspar dissolution and original data of Figure 9.

Sample	T/°C	T/K	1/T (K ⁻¹)	S _{K2O+SiO2+Al2O3} /%	D/%	lnD
L-2	130	403	0.0025	8.60	15.64	2.75
L-3	160	433	0.0023	15.53	28.24	3.34
L-4	190	463	0.0022	35.05	63.73	4.15
L-5	220	493	0.0020	45.89	83.44	4.42
L-6	250	523	0.0019	51.89	94.35	4.55

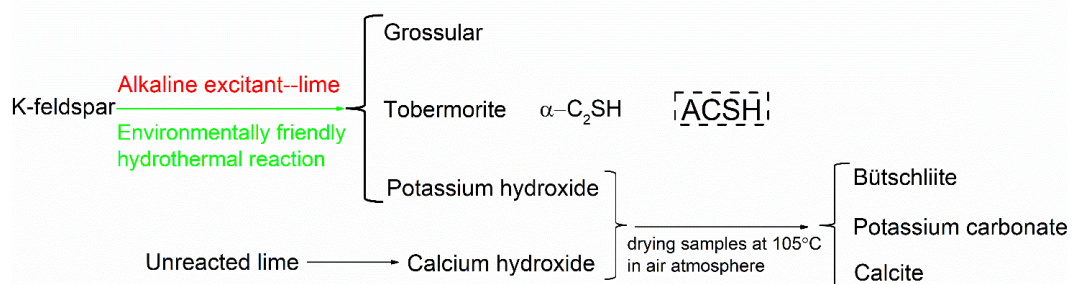


Figure S1. Flow chart of mineral phases during the K-feldspar and lime hydrothermal reaction.

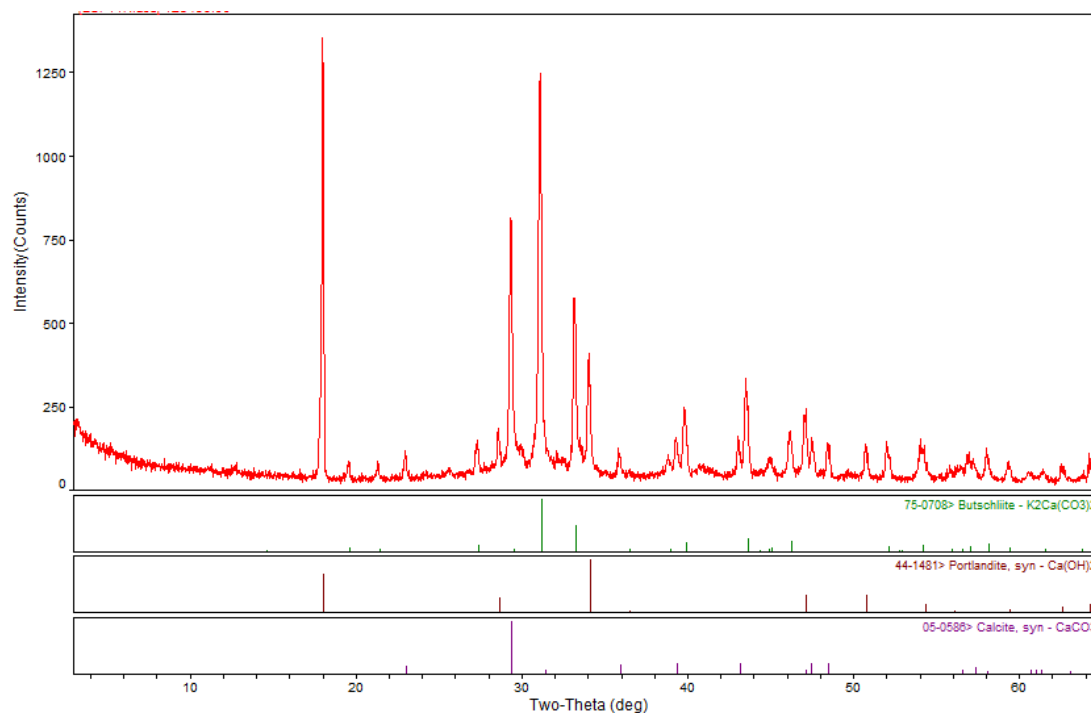


Figure S2. XRPD of the residue of the filtrated solutions of the samples from M-1 to M-9 dissolved in deionized water. The solid residue was obtained by mixing those filtrated solutions of the samples from M-1 to M-9 dissolved in deionized water and then vapping the mixed solution. The filtrated solution was obtained by adding a 1-g aliquot of each sample (nine samples, M-1 to M-9) to 100 ml of deionized water, agitating the sample for one hour, and filtering through the filter paper.

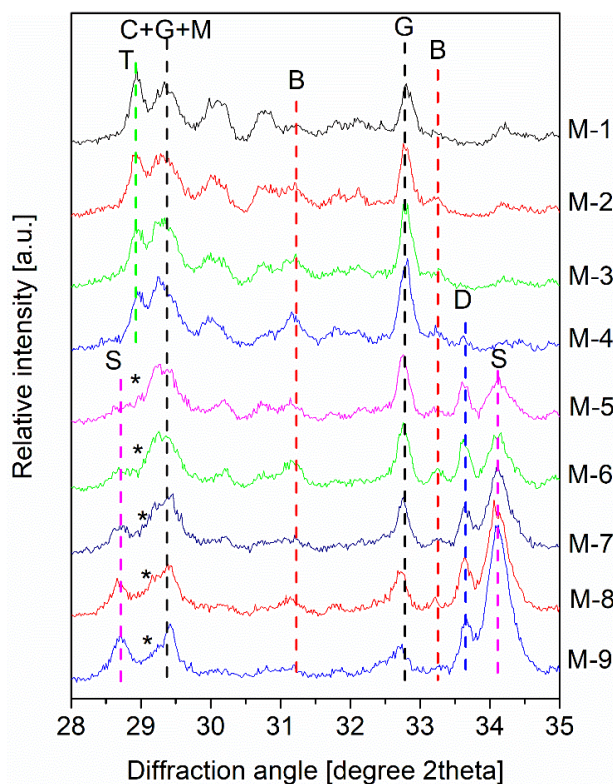


Figure S3. A magnified view of XRPD pattern of M-1 to M-9 from 28° to 35°. M—K-feldspar; S—calcium hydroxide; C—calcite; P—potassium carbonate; B—bütschliite; G—Grossular; D— α -C₂SH; T—tobermorite; *—amorphous calcium silicate hydrate.

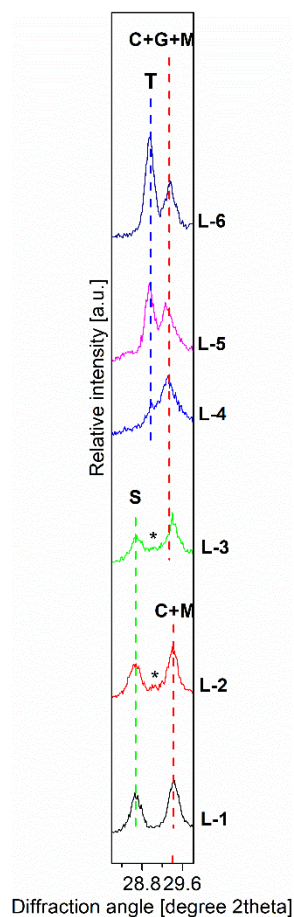


Figure S4. A magnified view of XRPD pattern of L-1 to L-6 from 28.2° to 29.8°. M—K-feldspar; S—calcium hydroxide; C—calcite; G—grossular; *—amorphous calcium silicate hydrate.

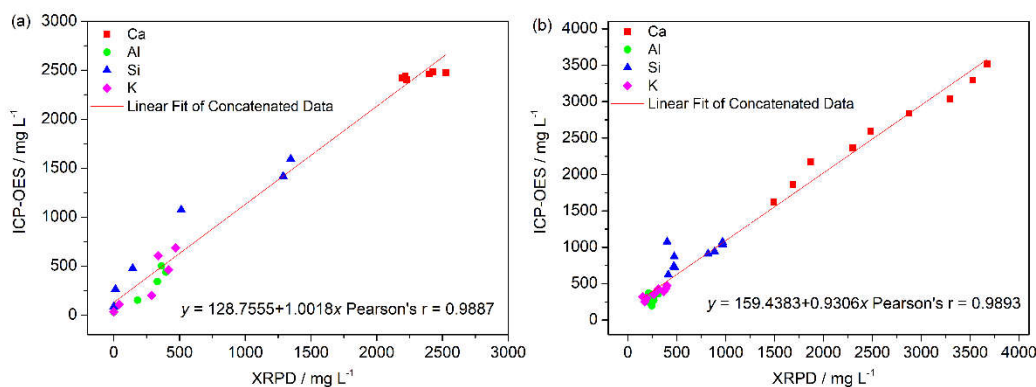


Figure S5. Element contents of ICP–OES vs. XRPD: (a) the hydrothermal reaction with reaction temperature; (b) the hydrothermal reaction with reactant ratio. ■Ca, ●Al, ▲Si, ◆K, — Linear fit (concatenating Ca, Al, Si, and K contents into a linear curve).

References

1. Liu, S.; Han, C.; Liu, J. Study of K-feldspar and lime hydrothermal reaction at 190 °C: phase, kinetics and mechanism with reaction time. *ChemistrySelect* **2018**, *3*, 13010–13016, doi:10.1002/slct.201802763.
2. Grew, E.S.; Locock, A.J.; Mills, S.J.; Galuskina, I.O.; Galuskin, E.V.; Halenius, U. Nomenclature of the garnet supergroup. *Am. Mineral.* **2013**, *98*, 785–810, doi:10.2138/am.2013.4201.